The Special Five-Membered Ring of Proline: An Experimental and Theoretical Investigation of Alkali Metal Cation Interactions with Proline and Its Four- and Six-Membered Ring Analogues

R. M. Moision and P. B. Armentrout*

Department of Chemistry, University of Utah, Salt Lake City, Utah 84112

Received: January 12, 2006

The interaction of the alkali metal cations, Li^+, Na^+, and K^+, with the amino acid proline (Pro) and its four- and six-membered ring analogues, azetidine-2-carboxylic acid (Aze) and pipecolic acid (Pip), are examined in detail. Experimentally, threshold collision-induced dissociation of the $M^+(L)$ complexes, where M = Li, Na, and K and L = Pro, Aze, and Pip, with Xe are studied using a guided ion beam tandem mass spectrometer. From analysis of the kinetic energy dependent cross sections, M^+-L bond dissociation energies are measured. These analyses account for unimolecular decay rates, internal energy of reactant ions, and multiple ion−molecule collisions. Ab initio calculations for a number of geometric conformations of the $M^+(L)$ complexes were determined at the B3LYP/6-311G(d,p) level with single-point energies calculated at MP2(full), B3LYP, and B3P86 levels using a 6-311+G(2d,2p) basis set. Theoretical bond energies show good agreement with the experimental bond energies, which establishes that the zwitterionic form of the alkali metal cation/amino acid, the lowest energy conformation, is formed in all cases. Despite the increased conformational mobility in the Pip systems, the Li^+, Na^+, and K^+ complexes of Pro show higher binding energies. A meticulous examination of the zwitterionic structures of these complexes provides an explanation for the stability of the five-membered ring complexes.

Introduction

Proline is a structural extreme among the 20 naturally occurring amino acids because its side chain binds to the amine end, forming both a secondary amine and a cyclic five-membered pyrrolidine ring. The ring significantly constrains the conformational flexibility of proline, such that it plays a unique role in the protein structure. It has been observed that proline cannot fit into the regular configuration of either α-helices or β-sheets, but its unique structural features may play a role in stabilization of the collagen triple helix.[1] It has also been shown that the intramolecular hydrogen binding in neutral gas-phase proline is much stronger than in other amino acids, largely because of the secondary amine.[2] An interesting anthropomorphic question is why nature chose a five-membered ring, rather than the more flexible, less constrained six-membered ring ubiquitous in nature.

Previous work in our lab[3,4] and others[5−10] have examined the binding of the sodium and potassium cation to glycine, the simplest amino acid. In these studies, the interaction of an alkali metal cation with even a single amino acid is shown to be quite complex. Despite its apparent simplicity, glycine has a number of low energy conformations arising from the internal degrees of freedom of the C−N, C−C, and C−O bonds, and the presence of intramolecular hydrogen bonding.[11] When glycine is bound to a metal ion, its polyfunctionality further complicates the picture as there are several functional groups where the metal ion can coordinate. Our results showed that the preferred binding of the alkali cation was the result of an energetic tradeoff, which differs for Na^+ and K^+. The geometry of the neutral glycine molecule distorts as the glycine molecule begins to solvate the charge of the metal cation. In the sodium case, glycine distorts into a slightly higher energetic conformation to bind as a bidentate ligand through the amine nitrogen and carboxylic acid carbonyl.[3] In the potassium case, the weaker binding, in particular to the amino group, means that the K^+ binds to the lowest energy conformation of glycine at the carboxylic acid.[4]

Here we examine the interaction of alkali cations with proline (Pro) and two of its analogues, azetidine-2-carboxylic acid (Aze) and pipecolic acid (Pip), which have four- and six-membered rings, respectively. Unlike glycine, these cyclic systems have very little conformational mobility to make use of when binding to an alkali cation. The constrained N−C−C−O dihedral angles in the cyclic amino acids provide insight into how much they can adapt to bind and solvate an alkali metal cation. Although both experimental[8−10,12] and theoretical[8,9,13] studies of alkali cations interacting with proline have been conducted, the subtle changes found by comparing the four-, five-, and six-membered rings should provide further insight into how amino acids can distort to accommodate an alkali metal cation. The recent spectroscopic work of Kapota et al.[10] establishes that, contrary to the other aliphatic amino acids, the most stable Na^+(Pro) complex is zwitterionic in the gas phase. By comparing proline to more (Aze) or less (Pip) rigid ring structures, we can address the properties that make the five-membered ring in proline unique. Absolute bond dissociation energies (BDEs) of the M^+-(L) (M^+ = Li^+, Na^+, K^+; L = Pro, Aze, Pip) complexes are measured using threshold collision-induced dissociation (TCID) in a guided ion beam tandem mass spectrometer. Theoretical calculations at the B3LYP/6-311G(d,p) level are carried out to provide structures, vibrational frequencies, and rotational constants needed for analysis of the TCID data. Experimental BDEs are compared to previous experimental values, where available, and to theoretical calculations performed for a number of possible $M^+(L)$ geometries at the MP2(full)/6-311+G(2d,2p),

10.1021/jp060230l CCC: $33.50
Published on Web 02/25/2006

B3LYP/6-311+G(2d,2p) and B3P86/6-311+G(2d,2p) levels using the B3LYP/6-311G(d,p) optimized geometries.

Experimental and Computational Section

General Experimental Procedures. Cross sections for CID of the metal−ligand complexes are measured using a guided ion beam tandem mass spectrometer that has been described in detail previously.[14,15] The metal−ligand complexes are produced in a discharge/flow tube (DC/FT) under conditions similar to those described previously.[3] Ions produced by this source are assumed to have their internal energy well described by a Maxwell−Boltzmann distribution of rovibrational states at 300 K.[16−21] Once formed, metal−ligand complexes are extracted from the source and mass selected using a magnetic momentum analyzer. The mass selected ions are decelerated to a well-defined kinetic energy and are focused into an radio frequency octopole ion guide that traps the ions radially.[22,23] This minimizes losses of the reactant and any product ions resulting from scattering. The octopole passes through a static gas cell containing xenon. Xenon is used as the collision gas for reasons described elsewhere.[24,25] After collision, the reactant and product ions drift to the end of the octopole where they are mass analyzed using a quadrupole mass filter. The ions are detected with a high voltage dynode, scintillation ion detector and the signal is processed using standard pulse counting techniques.

Ion intensities, measured as a function of collision energy, are converted to absolute cross sections as described previously.[14] The uncertainty in relative cross sections is about ±5% and that for the absolute cross sections is about ±20%. The ion kinetic energy distribution is measured to be Gaussian with a typical fwhm of 0.3 ± 0.1 eV (lab). Ion kinetic energies in the laboratory frame are converted to energies in the center-of-mass (CM) frame using standard formulas. All energies herein are reported in the CM frame unless otherwise noted.

Thermochemical Analysis. Threshold regions of the CID reaction cross sections are modeled using

$$\sigma(E) = \sigma_0 \sum_i g_i (E + E_i - E_0)^n / E \qquad (1)$$

where σ_0 is an energy-independent scaling factor, n is an adjustable parameter that describes the efficiency of collisional energy transfer,[15] E is the relative kinetic energy of the reactants, and E_0 is the threshold for CID of the ground electronic and rovibrational state of the reactant ion. The summation is over the rovibrational states of the reactant ions, i, where E_i is the excitation energy of each state and g_i is the fractional population of those states ($\Sigma g_i = 1$). Vibrational frequencies and rotational constants are taken from ab initio calculations, as detailed in the next section. The Beyer−Swinehart algorithm[26−28] is used to evaluate the density of the rovibrational states and the relative populations g_i are calculated for a Maxwell−Boltzmann distribution at 300 K.

Several systematic issues can obscure the interpretation of the data and must be taken into account during analysis to produce accurate thermochemical data. These include multiple reactant ion/neutral gas collisions and lifetime effects. Both of these effects are accounted for as described briefly below.

Equation 1 only models cross sections that represent products formed as the result of a single collision event. To ensure rigorous single collision conditions, data are collected at two or more pressures, generally about 0.16, 0.08, and 0.04 mTorr, and the cross sections are extrapolated to zero pressure prior to analysis. The need for this is illustrated in Figure 1, which shows an example cross section for the Na^+(Pro) system taken at 0.16 mTorr and after pressure extrapolation to 0.0 mTorr. At the 0.16 mTorr pressure, roughly 8% of the ions undergo a single collision and less than 1% undergo additional collisions. Even under these "single collision" conditions, the threshold shifts to energies that are lower than the zero-pressure extrapolated data by about 0.04 eV.

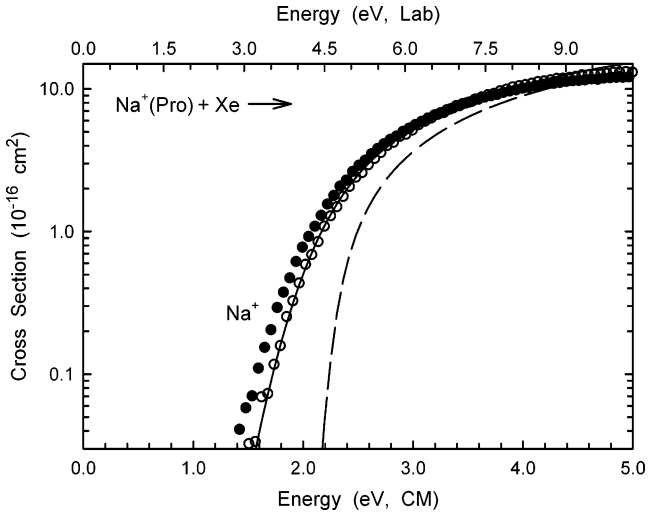

Figure 1. Cross sections for collision-induced dissociation of Na^+-(Pro) with Xe as a function of kinetic energy in the center-of-mass frame (lower *x*-axis) and the laboratory frame (upper *x*-axis). Data are shown for a xenon pressure of 0.16 mTorr (solid circles) and extrapolated to zero (open circles). The solid line shows the best fit to the extrapolated data using the model in eq 1 convoluted over the internal and kinetic energy distributions of the reactants. The dashed line shows the model cross section in the absence of experimental kinetic energy broadening for reactants with an internal energy of 0 K.

Dissociation is increasingly inefficient for large molecules with many internal modes where the internal energy can randomize. This results in ions that do not dissociate during the time scale of the experiment, $\sim 5 \times 10^{-4}$ s, and produces an observed threshold with an onset delayed from the thermodynamic limit, a kinetic shift, that becomes more noticeable as the size of the molecule increases. These kinetic shifts are estimated by incorporating Rice−Ramsperger−Kassel−Marcus (RRKM) statistical theory,[29] which predicts the unimolecular rate of dissociation of an energized molecule, into eq 1. Application of RRKM theory for analysis of CID thresholds using eq 1 has been described in detail elsewhere.[30] In all of the complexes studied here, we assume that the dissociation occurs with a loose transition state in the phase space limit (PSL) such that the transition states (TSs) are assumed to be product like. In the present work, the adiabatic 2-D rotational energy is treated using a statistical distribution with an explicit summation over the possible values of the rotational quantum number, as described in detail elsewhere.[30−32]

Overall, cross sections for a variety of alkali metal ion CID reactions have been reproduced using this model with good accuracy in the resulting thermochemistry.[31,33−40] Before comparison with the data, eq 1 is convoluted over the kinetic energy distributions of the reactants.[14,41] After convolution, model cross sections calculated using eq 1 are compared to the experimental reaction cross sections using a nonlinear least squares routine, and parameters σ_0, n, and E_0 are optimized. Estimates of the uncertainties associated with the measurements of E_0 are obtained from the range of threshold values determined for different data sets, variations associated with uncertainties in the calculated vibrational frequencies (±10% and a factor of 2

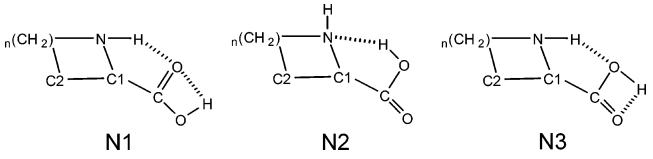

Figure 2. Schematic representations of the neutral conformations examined in the work: $n = 1$, Aze; $n = 2$, Pro; $n = 3$, Pip.

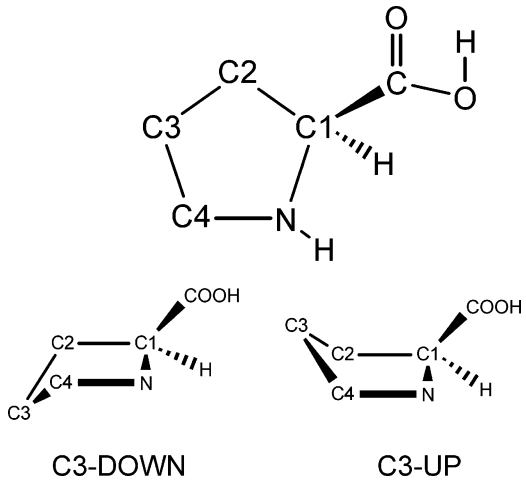

Figure 3. Nomenclature used in this paper for proline.

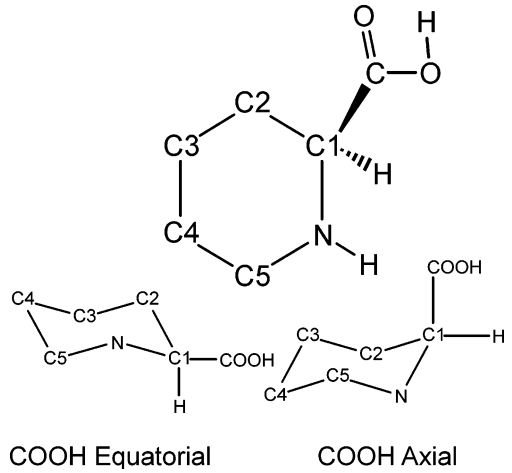

Figure 4. Nomenclature used in this paper for pipecolic acid.

for M^+-L modes), and the uncertainty in the absolute energy scale, 0.05 eV (lab). For analyses that include the RRKM lifetime effect, the uncertainty also includes that associated with increasing and decreasing the time assumed to be available for dissociation, $\sim 5 \times 10^{-4}$ s, by factors of 2.

The threshold energies for dissociation reactions determined by analysis with eq 1 are converted to 0 K bond energies by assuming that E_0 represents the energy difference between reactants and products at 0 K. This requires that there are no activation barriers in excess of the endothermicity of dissociation. This assumption has been shown to be generally valid for ion−molecule reactions[42] and for the heterolytic bond cleavage processes under consideration here.[43] We assume that the measured threshold energy is from the lowest energy complex to the lowest energy form of the neutral ligand, as discussed in more detail below. Given the length of time available for the complexes to dissociate ($\sim 5 \times 10^{-4}$ s), we believe this to be a reasonable assumption as the dissociating complex should be able to fully explore phase space thereby allowing the neutral ligand to reach its low energy conformation upon dissociation.

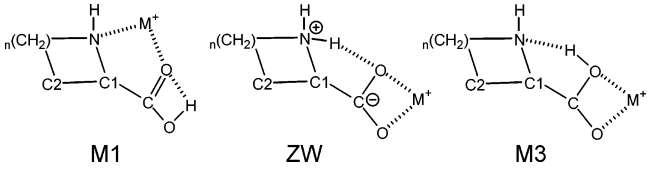

Figure 5. Schematic representations of the ground state and excited state conformations of $M^+(L)$ considered in this work: $M^+ = Li^+$, Na^+, K^+; $n = 1$, Aze; $n = 2$, Pro; $n = 3$, Pip.

Computational Details. Model structures, vibrational frequencies, and energetics for the neutral ligands and metalated complexes were obtained using Gaussian 03W.[44] Generally, the neutral ligands and metalated complexes have numerous geometric conformations with relative energies close to the lowest energy complex as discussed in detail below. In such cases, a number of conformations were generated to find the global minimum energy geometry as follows. A simulated annealing methodology using the AMBER suite of programs and the AMBER force field[45] was used to generate starting structures for higher level optimizations. All unique structures generated via simulated annealing were further optimized using nwchem[46] at the HF/3-21G level. For these alkali cation/single amino acid complexes, we have found that energies determined with this low level ab initio calculations show a higher correlation with energies produced at higher levels of theory than the relative energies from the AMBER force field. Because these are relatively small systems, the increased computational cost is acceptable. All unique structures from the HF/3-21G calculations within 30 kJ/mol of the lowest energy structure (~30 structures for each M^+(amino acid) complex) were further optimized using Gaussian 03W at the B3LYP/6-31G(d) level with the "loose" keyword to facilitate more rapid convergence.

All unique structures were then optimized at the B3LYP/6-311G(d,p) level. Rotational constants were obtained from the optimized structures and vibrational frequencies were also calculated at this level. When used in internal energy determinations or for RRKM calculations, the vibrational frequencies were scaled by 0.99.[47] This level of theory has been shown to give more accurate geometries and frequencies when compared to those found at the MP2(full)/6-31G(d) level.[47] Vibrational frequencies for the lowest energy complexes and free ligands are given in Table S1 and Table S2 lists their rotational constants. (For the sodium complexes, we also tested geometries optimized at the MP2(full)/6-31G(d) level and found that single-point energies, see below, were lower by ~0.5 kJ/mol at the MP2(full)/6-311+G(2d,2p) level and higher by about 3 kJ/mol at the B3LYP/6-311+G(2d,2p) and B3P86/6-311+G(2d,2p) levels. Because of these minor differences, such alternate geometry optimizations were not pursued for other systems.)

Single-point energies were calculated at the MP2(full), B3LYP, and B3P86 levels using the 6-311+G(2d,2p) basis set and the B3LYP/6-311G(d,p) geometries. Zero-point vibrational energy (ZPE) corrections were determined using the scaled vibrational frequencies calculated as described above. Basis set superposition errors (BSSE) were estimated using the full counterpoise method for the MP2 single-point energies[48] and ranged between ~9 kJ/mol for the Li^+ and Na^+ complexes to 5 kJ/mol in the K^+ complexes. For the B3LYP and B3P86 single-point energies, the BSSE corrections range between 1 and 3 kJ/mol for all structures examined here. This is consistent with previous observations by this lab[3,37] and others[49] that BSSE corrections for DFT calculations on alkali metal system are generally small. Feller and co-workers and Ohannesian and co-workers have previously commented that the full counterpoise

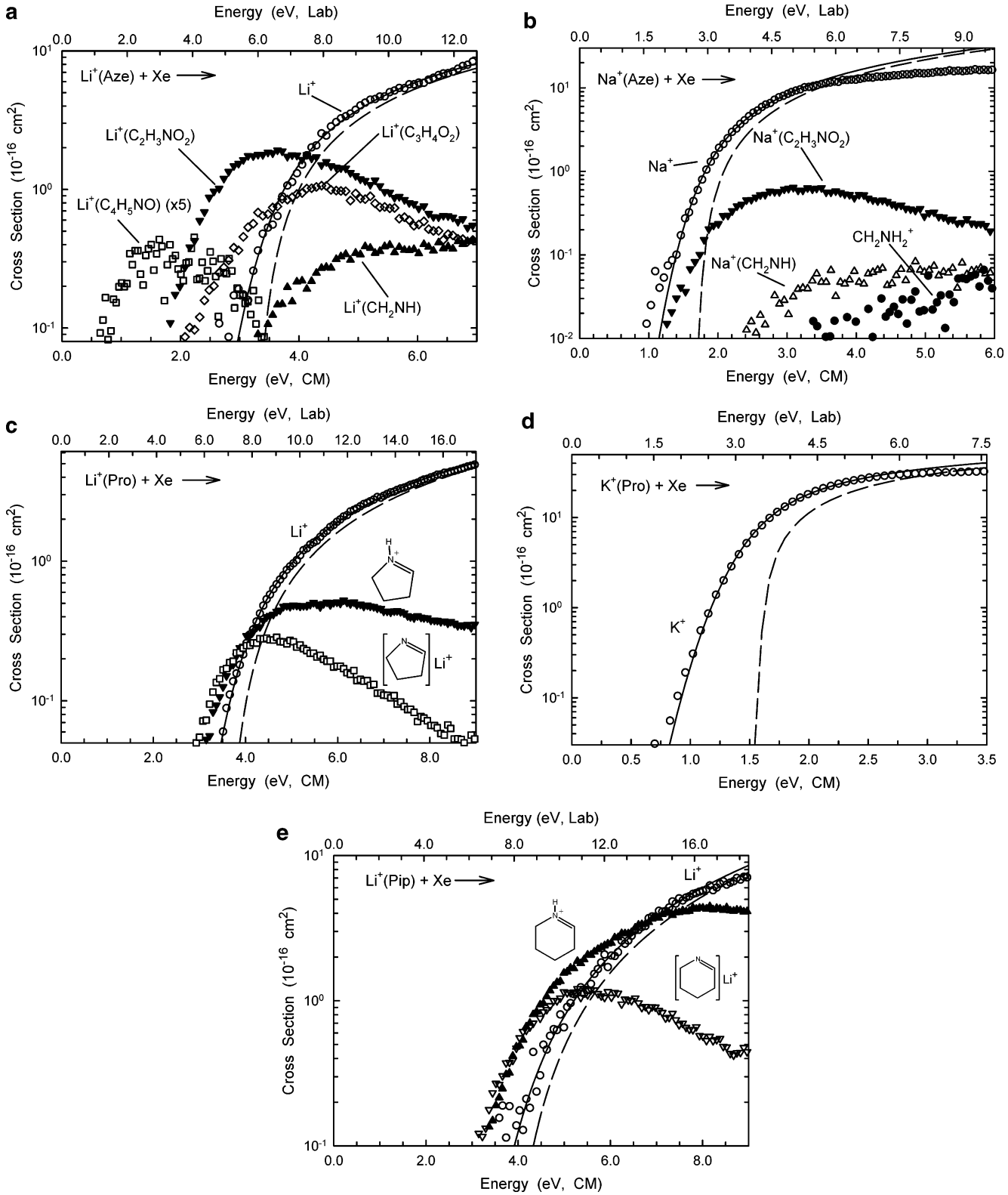

Figure 6. Zero pressure extrapolated cross sections for collision-induced dissociation of $M^+(L)$ with Xe in the threshold region as a function of kinetic energy in the center-of-mass frame (lower *x*-axis) and the laboratory frame (upper *x*-axis): (a) Li^+(Aze); (b) Na^+(Aze); (c) Li^+(Pro); (d) K^+(Pro); (e) Li^+(Pip). Aze = azetidine-2-carboxylic acid, Pro = proline, and Pip = pipecolic acid. Solid lines show the best fit to the data using the model of eq 1 convoluted over the neutral and ion kinetic and internal energy distributions. Dashed lines show the model cross sections in the absence of experimental kinetic energy broadening for reactions with an internal energy of 0 K.

approximation to BSSE can provide worse agreement with experiment than theoretical values without BSSE corrections.[6,50−52] Because of this tendency for BSSE to overcorrect for the MP2 calculations, it is possible that the "best" MP2 values most likely fall between the MP2 values with and without the inclusion of BSSE corrections, and both values are reported. All of the absolute binding energies obtained using DFT calculations reported here include BSSE corrections.

For the neutral Aze, Pro, and Pip structures, we have examined three possible conformations, each with slightly different intramolecular hydrogen binding. These structural motifs are shown in Figure 2. For Pro and Pip, these three motifs

are augmented by additional neutral structures with different ring structures and COOH locations as described above.

Figure 3 shows the nomenclature used for describing the Pro molecule. In this case, the α carbon is labeled C1 with the remaining ring carbons labeled C2−4 as the ring is navigated toward the amine nitrogen. The numbering nomenclature for carbons in the rings of Aze and Pip are analogous, e.g., Figure 4. The five-membered proline ring can "pucker" with one atom being out of plane relative to the other four. To describe this puckering in Pro structures, the 4 atoms in the ring with the dihedral angle closest to zero are considered to be "planar" and the remaining "out of plane" atom is designated either "up" (cis) or "down" (trans) relative to the location of the COOH group.

For Pip, the six-membered ring can form the conventional "boat" or "chair" structures. In all cases where the boat conformation is indicated, the structure is slightly twisted, where the hydrogens in the ring are in a nearly staggered conformation. We also indicate the location of the COOH group relative to the ring, either axial or equatorial, as shown in Figure 4.

When an amino acid is bound to an alkali metal cation, there are a number of possible binding conformations. We have examined these in detail for the case of Na^+ and K^+ with glycine.[3,4] Here, we focus on results for the complexes shown in Figure 5; the zwitterion (ZW) and charge solvated structures (M1 and M3). For some complexes of lithiated Pro and Pip, the M3 structure, where the alkali metal is bound to both oxygens of the carboxylic acid, optimizes to an M6 structure, where the metal is bound to only the carbonyl side of the carboxylic acid. For the present systems, we have examined a number of other complexes analogous to those detailed in our previous glycine work and have found them to be at least 20 kJ/mol higher in energy than the lowest energy complex. Many of these alkali cation/proline complexes have been examined previously by Talley et al.[53] However, at the MP2(full)/6-31G(d) level used by Talley for optimizing Pro structures, the M3 structure was found to collapse into the ZW structure. In the B3LYP/6-311G(d,p) calculations presented here, we find that two unique minima exist for the ZW and M3 structures.

Results

Cross Sections for Collision-Induced Dissociation. Experimental cross sections were obtained for the interaction of Xe with $M^+(L)$ for all nine alkali metal cation/amino acid combinations. These are shown in Figures 1 and 6a−e and Figure S1a−c in the Supporting Information. The only process observed for K^+(Aze), K^+(Pro), K^+(Pip), Na^+(Pro), and Na^+(Pip) is the loss of the intact ligand in the collision-induced dissociation (CID), reaction 2, as shown for the examples of Na^+(Pro) in Figure 1

$$M^+(L) + Xe \rightarrow M^+ + L + Xe \qquad (2)$$

and K^+(Pro) in Figure 6d. At high energies, reaction 2 is the most favorable process for all systems studied here. The Li^+(Pro) and Li^+(Pip) systems show two additional pathways that involve cleavage of the backbone C−COOH bond, as shown in Figure 6c,e. The lithium cation either stays with the carboxylic acid portion of the amino acid forming a neutral fragment, reaction 3 ($n = 3$ and 4), or remains with the ring to form a charged fragment, reaction 4 ($n = 3$ and 4). It is possible that the neutral products are LiOH + CO and H_2O + CO, respectively; however, ordinarily this would involve sequential processes in which either LiOH (H_2O) was lost first followed by CO loss, or vice versa. No ionic products corresponding to

$$Li^+(c\text{-}NH(CH_2)_nHC{-}COOH) + Xe \rightarrow c\text{-}(CH_2)_nCHNH^+ + LiCO_2H + Xe \qquad (3)$$

$$\rightarrow Li(c\text{-}(CH_2)_nCHN)^+ + CO_2H_2 + Xe \qquad (4)$$

such a sequential reaction were observed, although it is possible that their intensities are simply too small to detect in these experiments. In both the Li^+(Pro) and Li^+(Pip) cases, the thresholds for reactions 3 and 4 are roughly 0.5−0.7 eV lower than the loss of Li^+ in reaction 2, with reaction 4 having a slightly lower onset than reaction 3. In the case of Li^+(Pro), both of these pathways have maximum cross sections over 1 order of magnitude smaller than the loss of Li^+. Reactions 3 and 4 have much higher cross sections for Li^+(Pip) relative to Li^+(Pro), with reaction 3 having a maximum cross section ($\sigma_{max} = 4$ Å^2) only a factor of ∼2 lower in magnitude than reaction 2. In the Li^+(Pro) and Li^+(Pip) systems, reactions 4 show maximum cross sections at 4.5−5.0 eV that decrease at higher energies. The declines in the cross sections for reactions 4, energetically the most favorable processes, can be attributed to competition with reactions 3. This is consistent with the fact that reactions 4 require migration of an H atom to the CO_2H group, which probably involves a constrained transition state, whereas reactions 3 do not. It can be noted that reactions 3 and 4 are both backbone cleavages of the amino acids, which potentially has implications for the use of metalation in sequencing peptides by mass spectrometric methods.

In the cases of Li^+(Aze) and Na^+(Aze), Figure 6a,b, other fragmentation pathways are observed that imply cleavage across the four-membered ring, reactions 5 and 6 For Na^+(Aze),

$$M^+(c\text{-}NH(CH_2)_2HC{-}COOH) + Xe \rightarrow M^+(C_2H_3NO_2) + C_2H_4 + Xe \qquad (5)$$

$$\rightarrow M^+(CH_2NH) + C_3H_4O_2 + Xe \qquad (6)$$

reactions 5 and 6 both appear at thresholds higher than the loss of Na^+, by ∼0.2 and 1.5 eV, respectively. The loss of C_2H_4, reaction 5, has a maximum cross section of ∼0.7 Å^2. In contrast, the Li^+(Aze) system decomposes with a threshold for reaction 5 that appears roughly 1.5 eV lower in energy than loss of Li^+, and reaction 6 has a threshold only slightly above that for reaction 2. The Na^+(Aze) has an additional pathway, reaction 7. This is similar to reaction 6 with a proton transfer determining

$$Na^+(c\text{-}NH(CH_2)_2HC{-}COOH) + Xe \rightarrow NaC_3H_3O_2 + CH_2NH_2^+ + Xe \qquad (7)$$

the charged products and the detailed nature of the neutral product unclear, although propenoic acid with sodium substituted at the acid site seems likely.

Li^+(Aze) shows the most extensive fragmentation of the systems studied here with two additional reactions observed, reactions 8 and 9. The loss of water, reaction 8, has the lowest

$$Li^+(c\text{-}NH(CH_2)_2HC{-}COOH) + Xe \rightarrow Li^+(C_4H_5NO) + H_2O + Xe \qquad (8)$$

$$\rightarrow Li^+(C_3H_4O_2) + CH_2NH + Xe \qquad (9)$$

observed threshold at about 0.7 eV and a maximum cross section of only ∼0.09 Å^2. Its intensity decreases from 2.0 to 3.0 eV,

TABLE 1: Fitting Parameters of Eq 1, Threshold Dissociation Energies at 0 K, and Entropies of Activation at 1000 K for CID of M^+ (L) with Xe[a]

reactant[b]	σ_0	n	E_0 (eV)[c]	E_0(PSL) (eV)	$\Delta S^{\ddagger}_{1000}$(PSL) [J/(K mol)]
Li^+(Aze)	5.2(1.4)	1.8(0.3)	3.14(0.14)	2.60(0.14)	35.8(5)
Li^+(Pro)	2.4(0.8)	1.8(0.2)	3.66(0.10)	2.89(0.10)	51.1(6)
Li^+(Pip)	1.4(0.6)	2.4(0.2)	3.72(0.17)	2.82(0.17)	27.7(5)
Na^+(Aze)	16.2(3.2)	1.7(0.1)	1.97(0.05)	1.83(0.04)	34.7(5)
Na^+(Pro)	15.4(2.0)	1.4(0.1)	2.15(0.04)	1.93(0.05)	30.0(5)
Na^+(Pip)	29.8(1.8)	1.2(0.1)	2.52(0.06)	1.91(0.04)	27.4(5)
K^+(Aze)	50.7(3.8)	1.4(0.1)	1.42(0.05)	1.37(0.05)	29.6(5)
K^+(Pro)	57.7(4.3)	1.2(0.1)	1.59(0.04)	1.49(0.05)	38.6(6)
K^+(Pip)	69.0(4.0)	1.3(0.1)	1.56(0.05)	1.40(0.05)	24.9(5)

[a] Uncertainties are listed in parentheses. [b] Aze = azetidine-2-carboxylic acid. Pro = proline. Pip = pipecolic acid. [c] Does not include lifetime effects.

where it is no longer detected, presumably a result of competition with other more favorable processes, primarily reaction 5. Reaction 9 has an onset near 2.0 eV, roughly 1 eV lower than reaction 2, and a maximum cross section of 1.0 Å^2. This is clearly the analogue of reaction 6 in which the Li^+ is bound to the larger fragment of Aze. It seems probable that the analogue of reaction 9 occurs for dissociation of Na^+(Aze); however, this product would be difficult to observe in this system, as it should have a smaller intensity than the $Na^+(C_2H_3NO_2)$ product and is only 1 amu away.

Threshold Analysis. The model of eq 1 was used to analyze the thresholds for reaction 2 for the nine M^+(L) systems. Figures 1, 6, and S1 show that this model reproduces all experimental cross sections over a large range of energies (2−4 eV) and by at least a factor of 100 in magnitude. The optimum parameters for these analyses are provided in Table 1, which includes values for the thresholds, E_0, obtained with and without RRKM lifetime analysis. The magnitude of the kinetic shifts is lowest (0.05 eV) for K^+(Aze) and highest (0.90 eV) for Li^+(Pip). Kinetic shifts vary among the systems because they depend on the dissociation energy (higher E_0 values lead to larger kinetic shifts), the complexity of the system (larger systems have larger kinetic shifts), and the vibrational frequencies of both the cationized complex and the neutral ligand. It is possible that competition between the various product channels for the Li^+ systems may cause a shift in the threshold for reaction 2. This possibility is discussed further below.

From our analyses, we have also derived values for the entropy of dissociation, $\Delta S^{\ddagger}_{1000}$, which gives some idea of the looseness of the transition state. The PSL values, listed in Table 1, are in the range determined by Lifshitz[54] for the simple bond cleavage dissociations of several ions. This is reasonable considering that the TS is assumed to lie at the centrifugal barrier for the association of $M^+ + L$.

Theoretical Results: Neutrals. Structures of the three neutral ligands experimentally studied here were calculated as described above. For neutral Aze, the N2 structure, Figure 2 ($n = 1$), which contains only a single intramolecular hydrogen bond, is preferred by 2−5 kJ/mol at the MP2 level relative to the N1 conformation, Table 2. This is in contrast to the glycine case where the N1 structure containing both the N−H···O═C and O−H···O═C intramolecular hydrogen bonds has been found both experimentally and theoretically to be the energetic minimum.[11] The N3 conformation of Aze is 10−12 kJ/mol higher in energy relative to Aze N2. The N−C1−C2−C3 ring dihedral angle of the three neutral Aze conformations all have values within 0.4°, so ring distortions do not play a significant role in their relative stabilities. Examining the intramolecular hydrogen bond containing the amine nitrogen, N−H···O═C for N1, N···H−O−C for N2, and N−H···O−C for N3 offers insight into why the N2 structure is lowest in energy. The hydrogen bond lengths for the N1, N2, and N3 structures are 2.42, 1.95, and 2.37 Å with dihedral angles of 17°, 4°, and 24°, respectively. The gives the N2 structure, with the shortest and most planar hydrogen bond, an advantage over the N1 and N3 conformations, even though the latter have two hydrogen bonds each. The N1 and N3 structures have similar bond lengths and dihedral angles, but the N1 structure has both of its intramolecular hydrogen bonds coordinating to the carbonyl oxygen resulting in its energy being lower than the N3 structure.

TABLE 2: Theoretical Relative Energies of Neutral Structures

ligand[a]	bonding model[b]	ring structure[c]	COOH location[c]	relative energies (kJ/mol)[e] MP2	B3LYP	B3P86
Aze	N1			2.4	2.9	4.9
	N2			0.0	0.0	0.0
	N3			9.6	9.9	12.2
Pro	N1	C3-up		6.5	5.6	8.8
	N1	C4-up		6.5	4.7	8.2
	N2	C3-up		0.0	0.0	0.0
	N2	C4-up		3.8	2.3	3.1
	N3	C3-up		13.5	12.0	15.4
	N3	C4-up		13.8	14.6	16.8
Pip	N1	chair	equitorial	2.3	0.0	2.4
	N2	chair	axial	0.0	1.5	0.0
	N2	chair	equitorial	1.6	1.3	1.3
	N2	boat		17.0	16.0	14.6
	N3	chair	equitorial	2.6	1.3	3.7

[a] Aze = azetidine-2-carboxylic acid. Pro = proline. Pip = pipecolic acid. [b] Schematic of bonding models shown in Figure 2. [c] Ring nomenclature for Pro is shown in Figure 3 and for Pip in Figure 4. [d] All structures are geometry optimized and have zero-point energy corrections calculated at the B3LYP/6-311G(d,p) level. Final values are single-point energies at the levels indicated: MP2 = MP2(full)/6-311+G(2d,2p); B3LYP = B3LYP/6-311+G(2d,2p); B3P86 = B3P86/6-311+G(2d,2p).

For Pro, the N2 structure is again predicted to be the most stable. Although each atom in the five-membered ring can be situated in either an up or down position, resulting in 10 possible ring structures, all neutral structures optimized at the B3LYP/6-311G(d,p) level converge into either the C3-up or C4-up conformation. The C3-down structure for neutral Pro optimizes into the C4-up conformation primarily because this leaves the amine hydrogen staggered with respect to the hydrogens on the C4 carbon atom. The results for neutral Pro show that the C3-up ring conformation is favored over the C4-up ring conformation by 1−4 kJ/mol regardless of the intramolecular hydrogen bonds present (N1, N2, or N3 structures), Table 2. For all three structures, this is because the amine nitrogen in the C3-up ring conformation has a shorter N−H···C−O hydrogen bond distance and a more planar dihedral angle relative to the C4-up ring conformation. For example in the Pro N2 conformation, the N···HOC bond distances are 1.86 and 1.88 Å with dihedral angles of 0° and 6° for the C3-up and C4-up conformations, respectively. It is also notable that the N···HOC hydrogen bond in the N2 form of Pro is the shortest and most planar of all of the neutral structures studied here. Compare with 1.95 Å and 4° for the Aze N2 conformation, 1.98 Å and 16° for the Pip axial N2 conformation, and 1.95 Å and 13° for the Pip equatorial N2 conformation.

Our calculations (Table 2) find the Pro N2 C3-up structure is 5−9 kJ/mol lower in energy relative to the N1 C3-up structure. In contrast, matrix-isolation infared spectroscopy studies of Stepanian et al.[2] have reported that the N1 and N2

conformations for Pro exist in nearly equal proportions. It was found that only calculations with a high level of electron correlation, CCSD and CCSD(T), provided relative energies for these conformations in reasonable agreement with this experimental observation. Calculations using the MP2 and B3LYP methods were unable to predict with quantitative accuracy the relative energies of the neutral proline conformations, primarily because of the strength of the N···HO hydrogen bond. The MP2 and B3LYP calculations of Stepanian et al. found the N1 conformation to be 7−8 kJ/mol higher in energy than the N2 conformation, roughly the same as our calculations where the difference is 5−9 kJ/mol, Table 2. As in Aze, the N3 C3-up conformation in Pro is significantly higher in energy relative to the N1 and N2 conformations, lying 12−15 kJ/mol above N2.

In the Pip system, the N1, N2, and N3 bonding models with the ring in the chair conformation are all within 4 kJ/mol of each other at all levels of theory tried, Table 2. Calculations at the MP2 and B3P86 levels predict that the N2 conformation with the COOH in an axial position to be the energetic minimum, whereas B3LYP predicts the N1 structure to be the most stable, but the absolute differences are small, ≤3 kJ/mol. Given the experimental results of Stepanian et al.[2] for Pro, this may suggest that the true low energy conformation of Pip is N1. For the axial N2 conformation, the N···HOC bond length is 1.92 Å, slightly shorter than when the COOH is in the equatorial position at 1.98 Å. Despite the shorter N···HOC hydrogen bond length in the axial conformation, the N2 axial and equatorial conformations have nearly equal energies because the axial conformation generates greater distortions in the six-membered ring. This ring deformation is most evident by examining the H−C2−C1−H dihedral angles: axial N2, 46°; equatorial N2, 52°, N1, 53°, and N3, 57° (where 0° is fully eclipsed and 60° is completely staggered). This is unlike the Pro N2 conformation where the ring undergoes minimal distortions to maximize the amine intramolecular hydrogen bond. The energetic impact of having a distorted ring is more clearly evident when the Pip N2 conformation is placed into a twisted boat structure. Despite a shorter N···HOC bond distance of 1.87 Å, comparable to the Pro N2 conformations, the energy is considerably higher for the N2 boat, 15−17 kJ/mol, than any of the chair ring structures. Although the N1 and N3 conformations have two intramolecular hydrogen bonds, neither is as strong as that in the N2 conformations. In the Pip neutrals, the N3 amine hydrogen bond is slightly shorter than in the N1 conformation, 2.32 versus 2.42 Å, and the ring has the least amount of unfavorable steric interactions (e.g., consider the H−C2−C1−H dihedral angle noted above). The relative stability of the N3 conformation in the Pip neutrals is in stark contrast to the Aze and Pro systems where the N3 conformation are ∼10 and ∼13 kJ/mol higher than the lowest energy conformation, respectively. Overall, these various factors lead to the relative energies of the three conformations being similar for Pip, as noted above.

Theoretical Results: M^+(Aze). For all three alkali cation−Aze complexes studied here, the ZW form (Figure 5) is the most stable, Table 3. For the K^+(Aze) and Na^+(Aze) complexes, the ZW form is favored by over 10 kJ/mol over the M1 structure at all levels of theory, whereas the M1 structure is only 2−3 kJ/mol higher in energy for the Li^+ complex. By looking at the ZW and M1 structures in more detail, we see that the relative stabilization of the Li^+(Aze) M1 complex is the result of two factors: the lower stability of the hydrogen bond in the ZW structure and minimal extent of Aze distortion necessary to form the M1 complex. For the strongly bound, higher charge density Li^+ in the ZW structure, more electron density is required from the carboxylic acid to solvate the charge relative to Na^+ or K^+, leaving less electron density remaining to form the hydrogen bond. This is evident by observing the trend in the NH···OC hydrogen bond distance for the M^+(Aze) complexes: 1.85 Å for K^+, 1.90 Å for Na^+, and 1.95 Å for Li^+. Clearly, this intramolecular hydrogen bond weakens as Aze solvates an increasingly higher charge density metal ion.

TABLE 3: Theoretical Relative Energies of Metallated Aze[a]

metal	bonding model	relative energies (kJ/mol)[b] MP2	B3LYP	B3P86
Li^+	ZW	0.0	0.0	0.0
	M1	2.7	1.7	2.1
	M3	41.9	37.1	34.1
Na^+	ZW	0.0	0.0	0.0
	M1	10.6	11.7	11.1
	M3	24.1	25.9	22.0
K^+	ZW	0.0	0.0	0.0
	M1	10.4	12.8	13.5
	M3	11.1	13.2	10.9

[a] Aze = azetidine-2-carboxylic acid. [b] All structures are geometry optimized and have zero-point energy corrections calculated at the B3LYP/6-311G(d,p) level. Single-point energies are calculated at the levels indicated: MP2 = MP2(full)/6-311+G(2d,2p); B3LYP = B3LYP/6-311+G(2d,2p); B3P86 = B3P86/6-311+G(2d,2p).

To bind as a bidentate ligand through the amine nitrogen and carboxylic acid oxygen (M1 conformation), we have previously shown that the more flexible amino acid glycine (Gly) must distort to compromise between the energetic choices of maximizing binding strength and minimizing steric strain of the ligand.[3,4] In the Gly case, the ligand is free to rotate about the central C−C bond into a position that can fully take advantage of such an energetic compromise; however, the strained ring structure of Aze limits this rotation, forcing the metal ion to bind to relatively fixed positions of the amine nitrogen and carboxylic acid oxygen in the M1 complex. This is evident by examining the N···M^+···O═C dihedral angle formed in the pseudo five-membered ring of the M1 complex for the Aze and Gly complexes. For Aze, this angle does not change appreciably with the metal ion, being 4°, 3°, and 2° for K^+, Na^+, and Li^+, respectively. For Gly, the identical torsional angle shows much more variation at 15°, 10°, and 3°, respectively, with the strongly binding Li^+ inducing a near-planar geometry in the pseudo five-membered ring. When binding to the more flexible Gly ligand, the relatively weakly bound K^+ and Na^+ are unable to bring about the planarity of the N···M^+···O═C dihedral because of the size of the cation and the energetic cost of maintaining the hydrogen atoms on the amine and alpha carbon in an eclipsed conformation. In contrast, when these alkali metals bind to the highly constrained Aze, the K^+ and Na^+ are forced to attach to the amine nitrogen and carboxylic acid oxygen in an unfavorable, near-planar conformation. Contrast this to the Li^+, where the constraint imposed by the four-membered ring in Aze results in the N···M^+···O═C dihedral angle being nearly identical to that of the Gly system. The net effect of these two factors is to leave the M1 and ZW forms nearly equal in energy for the Li^+-(Aze) complex, whereas the ZW form is clearly favored for the Na^+ and K^+ ions.

Theoretical Results: M^+(Pro). For all akali cation−Pro complexes studied here, the ZW form was found to be the most stable, Table 4, by at least 9 kJ/mol. As with the neutral, despite 10 possible ring structures from the up/down puckering, all variations for all bonding models collapsed to one of two ring structures, C3-up and C3-down when optimized at the B3LYP/

TABLE 4: Theoretical Relative Energies of Metallated Pro[a]

metal	bonding model	ring structure[b]	relative energies (kJ/mol)[c] MP2	B3LYP	B3P86
Li^+	ZW	C3-up	0.0	0.0	0.0
	ZW	C3-down	3.8	1.5	2.4
	M1	C3-up	14.1	12.6	12.9
	M1	C3-down	11.2	9.1	9.7
	M6	C3-up	44.8	40.9	36.7
Na^+	ZW	C3-up	0.0	0.0	0.0
	ZW	C3-down	4.6	2.1	3.0
	M1	C3-up	25.6	23.5	25.3
	M1	C3-down	21.9	21.0	21.5
	M3	C3-up	25.9	26.9	23.0
	M3	C3-down	29.6	28.8	25.8
K^+	ZW	C3-up	0.0	0.2	0.1
	ZW	C3-down	5.3	0.0	0.0
	M1	C3-up	25.5	23.5	24.8
	M1	C3-down	22.4	21.4	21.1
	M3	C3-up	14.7	13.1	9.9
	M3	C3-down	18.2	14.1	12.4

[a] Pro = proline. [b] Ring nomenclature for proline shown in Figure 3. [c] All structures are geometry optimized and have zero-point energy corrections calculated at the B3LYP/6-311G(d,p) level. Single-point energies are calculated at the levels indicated: MP2 = MP2(full)/6-311+G(2d,2p); B3LYP = B3LYP/6-311+G(2d,2p); B3P86 = B3P86/6-311+G(2d,2p).

6-311G(d,p) level. By looking down the C1−N axis in the C3-up and C3-down conformations, we note that the atoms bound to the C1 and N ring locations are forced into nearly planar eclipsed conformations; e.g., the H−C1−N−H torsional angle is under 1° in both the Na^+(Pro) ZW C3-up and C3-down conformations. It is the strength of the N−H···O═C intramolecular hydrogen bond that drives these strongly preferred ring puckering locations for M^+(Pro) complexes. As structures starting with other puckering locations begin to optimize, the N−H···O═C hydrogen bond shortens and becomes more planar, which forces the ring into forming only the C3-up and C3-down conformations.

One might expect these puckering isomers to have indistinguishable relative energetics; however, the differences are systematic and range from 0 to 5 kJ/mol, with C3-up generally preferred for ZW and M3/M6 structures and C3-down preferred for M1. In a five-membered ring, the location of the puckering causes the atoms or groups bound to the ring locations on the far side of the ring (those two ring positions across from the puckering location) to undergo a subtle distortion. This causes the substituents on the same side of the ring as the pucker to come closer together and those on the opposite side to be splayed farther apart. For instance, in neutral cyclopentane with a C3-up pucker location, the up hydrogens on C1 and C5 are 0.06 Å closer relative to the down hydrogens. With the C3 pucker in proline, a similar trend is observed in the N and C1 substituents. For instance, the N−H and C1−H hydrogens on the opposite side in Na^+(Pro) ZW are 2.300 and 2.250 Å apart in C3-up and C3-down conformations, respectively, whereas the N−H and C1−C atoms on the "up" side are 2.207 and 2.247 Å apart, respectively. This results in a shortening of the N−H···O═C hydrogen bond distance in the C3-up by an average of 0.047 ± 0.013 Å relative to the C3-down complex. An examination of the N−H···O═C torsional angle in the C3-up and C3-down ZW conformations also explains how the C3-up conformations further gains an energetic advantage. For C3-up, this hydrogen bond is nearly planar with the torsional angle ranging from 0.5 to 0.8° for different metal ions, but the C3-down is less planar, with angles ranging from 1.9 to 2.5°. For the Na^+(Pro) complex, the transition state between the C3-up and C3-down conformations, calculated using the QST2 search algorithm[55] at the B3LYP/6-311G(d,p) level, is the C1 up conformation, which lies 10 kJ/mol higher in energy relative to the C3-up complex.

TABLE 5: Theoretical Relative Energies of Metallated Pip[a]

metal	bonding model	ring structure[b]	COOH location[b]	relative energies (kJ/mol)[c] MP2	B3LYP	B3P86
Li^+	ZW	chair	equatorial	0.0	0.0	0.0
	ZW	chair	axial	0.4	2.9	2.0
	ZW	boat		13.2	15.4	13.6
	M1	chair	equatorial	13.7	12.7	12.7
	M1	chair	axial	14.8	14.7	13.9
	M3	chair	axial	50.6	50.6	44.6
	M6	chair	equatorial	56.1	51.0	47.8
Na^+	ZW	chair	equatorial	0.4	0.0	0.0
	ZW	chair	axial	0.0	2.1	0.8
	ZW	boat		13.2	11.5	10.0
	M1	chair	equatorial	20.8	21.8	19.4
	M1	chair	axial	20.5	22.5	21.3
	M3	chair	axial	30.3	31.9	26.8
K^+	ZW	chair	equatorial	1.4	0.0	0.3
	ZW	chair	axial	0.0	0.9	0.0
	ZW	boat		9.6	11.3	9.4
	M1	chair	equatorial	18.7	20.6	18.7
	M1	chair	axial	17.8	21.8	21.1
	M3	chair	equatorial	22.0	21.7	19.7
	M3	chair	axial	16.1	17.0	13.9

[a] Pip = pipecolic acid. [b] Ring nomenclature for Pip shown in Figure 4. [c] All structures are geometry optimized and have zero-point energy corrections calculated at the B3LYP/6-311G(d,p) level. Single-point energies are calculated at the levels indicated: MP2 = MP2(full)/6-311+G(2d,2p); B3LYP = B3LYP/6-311+G(2d,2p); B3P86 = B3P86/6-311+G(2d,2p).

Theoretical Results: M^+(Pip). As with Aze and Pro, the M^+(Pip) complexes studied here have ZW as the most stable form, Table 5, with the M1 and M3/M6 structures >12 kJ/mol higher in all cases. For all three alkali metals, the relative energies of the COOH in the axial or equatorial position are nearly identical (within 3 kJ/mol). This isoenergetic behavior is a bit surprising as the axial conformation in methyl cyclohexane is ∼7 kJ/mol higher in energy relative to the equatorial conformation, a difference that can be attributed to unfavorable steric interactions of the axial substituent with the other axial hydrogens in the ring. However, in the M^+(Pip) complexes, a negatively charged carboxylic acid in an axial position could result in attractive interactions with the axial hydrogens. In addition, the axial COOH position results in a more planar and shorter N−H···O═C hydrogen bond. For all three metal ions, the length of the H···O bond in the axial conformations is 0.243 ± 0.002 Å shorter than this bond length in the equatorial conformation, which allows the axial conformation to form a stronger stabilizing hydrogen bond. It should be noted that neither the axial nor equatorial conformation has a particularly planar N−H···O═C hydrogen bond torsional angle, with the angle averaging 23 ± 1° for the axial and 38 ± 3° for the equatorial conformations. The N−H···O═C hydrogen bond in the latter conformation actually lies between the two amine hydrogens, but for all metal complexes, one of these hydrogen bonds is significantly longer (2.216 ± 0.064 Å vs 2.612 ± 0.029 Å) and less planar (dihedral angles of 38 ± 3° vs 67 ± 3°).

It is also of note that the "boat" ZW configuration is relatively low in energy for all three metalated systems. This stabilization is again the result of the N−H···O═C hydrogen bond being shorter, 1.81 ± 0.07 Å (ZW boat) vs 1.97 ± 0.07 Å (ZW chair-axial), and more planar, 3.9 ± 0.1° (ZW boat) vs 23.0 ± 1.4° (ZW chair-axial). The shorter and more planar hydrogen bond results in the ZW boat form being only 9−15 kJ/mol higher in energy than the ZW chair forms. For comparison, unfavorable

steric interactions in an unsubstituted cyclohexane cause the boat structure to be ~25 kJ/mol higher in energy relative to the chair form.[56] The comparison of bond length and planarity above shows that to maximize the strength of this intramolecular hydrogen bond, the six-membered ring must adopt the higher energy boat conformation. The stabilization offered by the stronger hydrogen bond is unable to overcome the unfavorable ring distortions in the boat form. Thus, despite the potential flexibility offered by the six-membered ring, for the ZW complex, the strength of the hydrogen bond is actually limited by the conformations of the ring.

Transition State for Conversion Between Zwitterionic and Charge Solvated Forms. Our theoretical work concentrates on characterizing the lowest energy structures of the various complexes studied experimentally to provide molecular parameters for our analysis and theoretical energies for comparison to the experimental results. In addition, much of the potential energy surface for the M^+(Pro) ($M^+ = Li^+$, Na^+, and K^+) systems has been studied systematically by Marino, Russo, and Toscano (MRT),[13] and one imagines that the M^+(Aze) and M^+(Pip) are qualitatively similar. However, MRT were unable to locate the transition state for interconversion of the ZW and M3 forms of M^+(Pro). As this interconversion is important in understanding several experimental results, see below, we reexamined this aspect of the potential energy surface and successfully employed the synchronous transit-guided quasi-newton (STQN) method of Schlegel and co-workers[55,57] to find this transition state for all nine systems examined here. For these transition states, the B3LYP/6-311G(d,p) level of theory was used; however, to be sure that differences in basis set were not responsible for the location of the transition state result, we also utilized the 6-311++G(d,p) basis used by MRT in the case of all proline complexes. Comparable results were found for both basis sets.

As noted above, the M3 complex lies higher in energy than the ZW isomer for most of the nine systems. The exception is the Li^+(Pro) complex, where the M3 complex is unstable and a monodentate M6 structure is formed instead, as noted above. For systems in which the transition state lies between the M3 and ZW isomers, a transition state was found in which the imaginary frequency corresponds simply to the motion of the hydrogen atom between the O and N centers. For all three metalated proline complexes examined here, such a transition state exists for both the C3-up and C3-down forms. Interestingly, although these transition states can be located on the potential energy surface and clearly have energies above the M3 forms, the addition of zero-point energy (ZPE) causes the energy of the transition state to fall below that for the M3 complex. For example, in the Na^+(Pro) system, the transition state lies 2 kJ/mol higher than the M3 complex without the addition of ZPE and 4 kJ/mol lower when ZPE is included. Inclusion of ZPE has the same effect for the relative enthalpies at 298 K. At the MP2/6-31G(d) level for Na^+(Pro), the M3 complex is unstable as there is no transition state with or without the addition of ZPE. Thus, for all of the complexes except Li^+(Pro), the M3 complex spontaneously collapses to the ground-state ZW conformation once zero-point energies are included.

In the case of Li^+(Pro), the transition state between M6 and ZW involves transfer of the proton as well as motion of the Li^+ cation as it moves from binding the carboxyl oxygens monodentate (M6) to bidentate (ZW). Figure 7 shows this coordinated motion of the M6 to ZW transition calculated at the B3LYP/6-311G(d,p) level. Starting from the M6 complex ($r_{NH} = 1.02$ Å, $r_{OH} = 1.72$ Å), where the Li^+−O-C angle is ~155°, the Li^+ ion begins to swing toward the OH as this angle decreases and there is a small increase in energy. At an angle of ~100° ($r_{NH} = 1.05$ Å, $r_{OH} = 1.64$ Å), the energy begins to decrease as the transient M3 complex forms. Because there is no barrier for transition from the M3 to ZW complex, the energy begins to abruptly decrease as the hydrogen transfers to the nitrogen at an Li^+−O−C angle of around 90° ($r_{NH} = 1.84$ Å, $r_{OH} = 1.04$ Å).

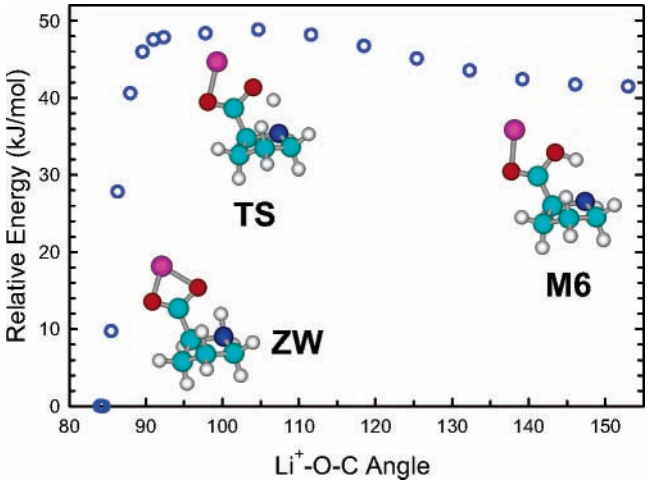

Figure 7. Energy profile of the M6 to ZW transition for Li^+(Pro) as a function of the Li^+−O-C angle calculated at the B3LYP/6-311G-(2d,2p) level.

Discussion

Comparison between Theory and Experiment. In the following, all theoretical bond energies cited are adiabatic; i.e., they presume that the complexes dissociate to M^+ + the amino acid in its lowest energy conformation, a nonzwitterionic form. We find that agreement between theory and experiment for the nine complexes examined here is quite good. A comparison of the experimental binding energies to the ZW and lowest energy charge solvated (CS) complex, Table 6 and Figure 8, shows that for all levels of theory examined here the ZW values give better agreement with experimental values relative to the CS values. All levels of theory give comparable mean absolute deviations (MADs) of 6−8 kJ/mol for the ZW structures, but 11−21 kJ/mol for the CS structures. The former deviations are roughly the magnitude of the experimental uncertainties. Therefore, we conclude that our experimental values correspond to the lowest energy ZW structures in all cases. For the sodiated complex of proline, this is consistent with the spectroscopic findings of Kapota et al.,[10] although none of the other complexes studied here have been examined spectroscopically to date.

A more careful examination of the different levels of theory reveals that agreement with experimental values is excellent for all three potassium systems (MAD = 3.4 ± 0.5 kJ/mol), Table 6 and Figure 8. For the sodium complexes, the experimental results fall between the MP2 results with (MAD = 2.3 ± 0.7 kJ/mol) and without (MAD = 6.9 ± 0.8 kJ/mol) BSSE corrections and are within experimental error of the B3P86 values (MAD = 3.2 ± 0.4 kJ/mol). As observed previously for sodium ion complexes,[58] the B3LYP values are systematically high (MAD = 10.6 ± 0.8 kJ/mol). The worst agreement with experiment occurs for the Li^+ complexes, where agreement between theory and experiment is relatively good for Li^+(Aze), within experimental error for Li^+(Pip), and theory underestimates the value for Li^+(Pro). Such underestimations are a common discrepancy for lithiated complexes[39,59−61] and may

TABLE 6: Experimental and Theoretical Binding Energies at 0 K for M^+(L) Complexes

	experiment		theory[c] MP2		MP2 (+BSSE)		B3LYP		B3P86		
complex[a]	this work[b]	lit.	ZW	CS[d]	ZW	CS[d]	ZW	CS[d]	ZW	CS[d]	lit.
Li^+(Aze)	250(14)		251	249	242	239	256	255	249	247	
Li^+(Pro)	279(10)	229(13)[f,g]	258	247	249	238	263	255	255	245	264−274[e]
Li^+(Pip)	272(16)		264	250	255	241	272	259	262	249	
Na^+(Aze)	177(5)		183	172	174	163	187	175	180	168	
Na^+(Pro)	186(4)	194(8),[g,h] 173(12)[g,i]	193	171	184	162	196	175	189	167	193,[g,h] 189, 162,[g,i] 193−200[e]
Na^+(Pip)	184(6)		192	172	183	162	196	174	188	167	
K^+(Aze)	132(5)		135	124	130	120	134	121	134	123	
K^+(Pro)	144(4)		145	130	140	126	141	128	139	130	142,[g,j] 144−150[e]
K^+(Pip)	135(5)		142	126	137	121	142	124	140	126	
MAD			7(6)	13(9)	8(10)	21(10)	7(5)	11(6)	6(7)	15(10)	

[a] Uncertainties are listed in parentheses. [b] Aze = azetidine-2-carboxylic acid. Pro = proline. Pip = pipecolic acid. [c] All structures are geometry optimized and have zero-point energy corrections calculated at the B3LYP/6-311G(d,p) level. MP2 = MP2(full)/6-311+G(2d,2p); B3LYP = B3LYP/6-311+G(2d,2p); B3P86 = B3P86/6-311+G(2d,2p). All values include corrections for BSSE. [d] CS indicates the theoretical bond energy to the lowest energy non-Zwitterionic conformation, ether M1 or M3 in Tables 3−5. [e] Marino, Russo, and Toscano[13] report a number of binding energies using a variety of DFT methods. For brevity, only the highest and lowest are shown here. [f] Feng, Gronert, and Lebrilla.[66] [g] Value adjusted to ΔH_0 using data in Table 7. [h] Kish, Ohanessian, and Wesdemiotis.[8] [i] Gapeev and Dunbar.[9] [j] Lau et al.[7]

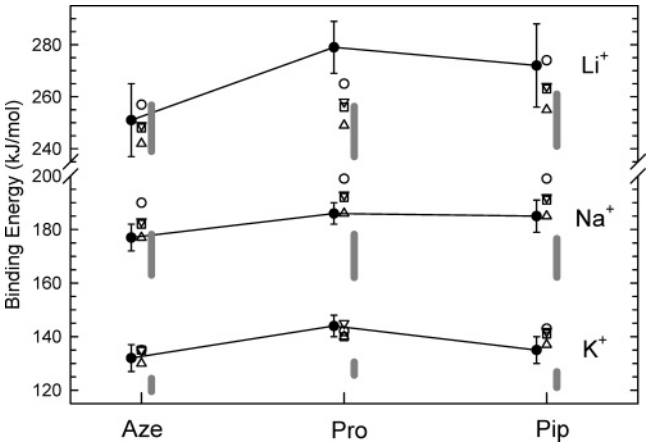

Figure 8. Experimentally measured 0 K bond dissociation energies (in kJ/mol) for the nine systems studied (closed circles) and ab initio calculated 0 K bond dissociation energies (open symbols) using MP2/6-311+G(2d,2p)//B3LYP/6-311G(d,p) with and without BSSE corrections (triangles and inverted triangles, respectively), B3LYP/6-311+G(2d,2p)//B3LYP/6-311G(d,p) (circles), and B3P86/6-311+G(2d,2p)//B3LYP/6-311G(d,p) (squares). The gray box shows the range of theoretical 0 K bond dissociation energies calculated at the levels of theory stated above for the lowest energy nonzwitterionic structure. Vertical error bars are for experimental values. Aze = azetidine-2-carboxylic acid, Pro = proline, Pip = pipecolic acid.

be a result of the difficulty that theory has with describing a metal−ligand bond with a high degree of covalency, especially in a case involving chelation. Work in progress[62] suggests that these theoretical limitations may be overcome by considering core polarization effects on the Li^+ ion and by extrapolating to the complete basis set limit, but this advanced protocol has not yet been developed sufficiently to consider in the present work. However, recent results suggest that the G3 protocol[63] does a reasonable job of addressing these core polarization effects.[62] G3 calculations on the Li^+(Pro) system give a bond energy of 261 kJ/mol, comparable to our B3LYP value and just below the experimental value of 279 ± 10 kJ/mol reported here.

Alternatively, there may be particular difficulties with the interpretation of the CID threshold for the lithium systems. For the three Li^+ systems studied here, all cross sections have fragmentation products with thresholds occurring at lower energies than the loss of Li^+, Figures 6a,c,e, and these are particularly prominent in the Aze and Pip systems. It is possible that these product channels are in competition with the Li^+ loss channel, which could result in the experimental threshold energy being high. However, we would expect the magnitude of such competitive shifts to be the smallest for the Li^+(Pro) system, where the competitive products are smallest and have the highest thresholds, compared to the Li^+(Aze) and K^+(Aze) systems, whereas the discrepancy between experiment and theory is largest for Li^+(Pro). Another possible limitation in the data could occur if the ZW and M1 isomers are both being formed experimentally. However, the presence of the higher energy isomer would lead to an experimental value lower than theoretically predicted, in contrast to observation. Finally, as mentioned above, our modeling assumes a PSL or loose transition state, whereas for the tightly bound Li^+ ZW structures, a tighter transition state may provide a more appropriate description of the dissociation behavior. Such a change in the modeling would result in a larger kinetic shift and therefore a lower threshold energy, which could make the agreement between experiment and theory better. At this point, it is unknown whether the interpretation of the data or deficiencies in theory are most responsible for the discrepancies observed.

Conversion to 298 K Values. Because many previous literature values and experimental conditions are tabulated at 298 K, we convert our 0 K bond energies to 298 K bond enthalpies and free energies. The enthalpy conversions and entropy contributions are calculated using standard formulas and the vibrational and rotational constants determined at the B3LYP/6-311G(d,p) level of theory. Uncertainties in these values are determined by 10% variations in most molecular constants in addition to scaling the metal−ligand frequencies by a factor of 2 in either direction. The calculated conversion factors and resultant ΔH_{298} and ΔG_{298} values are reported in Table 7.

Comparison to Experimental Literature Values. The Na^+(Pro) system has been previously studied experimentally by Kish, Ohanessian, and Wesdemiotis (KOW),[8] Gapeev and Dunbar (GD),[9] and Kapota, Lemaire, Maître and Ohanessian (KLMO).[10] KOW report an experimental ΔH_{298} obtained using the kinetic method of 196 ± 8 kJ/mol, within experimental error of our value of 188 ± 4 kJ/mol. The KOW affinities are anchored to an absolute value using the alanine (Ala) amino acid of 166.8 kJ/mol, which was determined from kinetic method experiments using theoretical 298 K sodium ion affinities of acetamide, *N*-methylacetamide, and *N*,*N*-dimethylacetamide as

TABLE 7: Enthalpies and Free Energies of M^+(L) Binding at 0 and 298 K in kJ/mol[a]

system[b]	ΔH_0[c]	$\Delta H_{298} - \Delta H_0$	ΔH_{298}	$T\Delta S_{298}$	ΔG_{298}
Li^+(Aze)	250(14)	2.6(0.2)	253(14)	30(5)	223(15)
Li^+(Pro)	279(10)	3.0(0.2)	282(10)	34(5)	248(11)
Li^+(Pip)	272(16)	2.3(0.1)	274(16)	30(5)	244(17)
Na^+(Aze)	177(5)	2.6(0.2)	179(5)	35(5)	144(7)
Na^+(Pro)	186(4)	1.7(0.1)	188(4)	33(5)	155(6)
Na^+(Pip)	184(6)	1.3(0.1)	186(6)	31(5)	154(8)
K^+(Aze)	132(5)	0.8(0.1)	133(5)	30(5)	104(7)
K^+(Pro)	144(4)	1.1(0.1)	145(4)	31(5)	114(6)
K^+(Pip)	135(5)	0.7(0.1)	136(5)	30(5)	106(7)

[a] Uncertainties are listed in parentheses. [b] Aze = azetidine-2-carboxylic acid. Pro = proline. Pip = pipecolic acid. [c] Calculated using standard formulas and molecular constants given in Tables 1S and 2S.

references. The range of effective temperatures in these studies was 413 ± 45 K, leading to uncertainties of 1−6 kJ/mol in the determination of relative affinities and ± 8 kJ/mol in the absolute affinities. As another point of reference, KOW also obtained a 298 K value for Na^+(Gly) that is slightly lower, 161 ± 8 kJ/mol, but within experimental error of our previously published Na^+(Gly) value of 166 ± 6 kJ/mol at 298 K.[3] If our experimental value for Na^+(Gly) was used to anchor the sodium ion affinity scale of KOW, this would yield an Na^+(Pro) affinity of 201 ± 8 kJ/mol, 13 kJ/mol higher than the experimental value reported here, and in worse agreement than the value obtained using the Na^+(Ala) anchor. An alternate way of comparing these results is to note that the relative KOW measurements find a difference in sodium ion affinities of Gly and Pro of 35 ± 4 kJ/mol, whereas our TCID studies find 22 ± 7 kJ/mol.

The Na^+(Pro) system has also been studied previously by GD using ligand exchange equilibria.[9] They find a difference in the sodium cation affinities of Gly and Pro of 14.6 ± 6 kJ/mol, within experimental error of our difference of 22 ± 7 kJ/mol, but much smaller than the relative value from KOW of 35 ± 4 kJ/mol. In contrast, theory seems to agree slightly better with the KOW result, giving an average difference of 32 ± 1 kJ/mol at the B3LYP, B3P86, and MP2(full) levels of theory.[3] GD report an absolute ΔH_{298} value for Na^+(Pro) of 175 ± 12 kJ/mol when their scale is anchored to the Na^+(Gly) BDE of 161 kJ/mol from KOW. This value is 21 kJ/mol below the value of KOW for Na^+(Pro), but within experimental error of our ΔH_{298} value of 188 ± 4 kJ/mol. If GD's scale is instead anchored to our previously published Na^+(Gly) value of 166 ± 6 kJ/mol, this results in a Na^+(Pro) BDE of 180 ± 12 kJ/mol, in very good agreement with our ΔH_{298} value. Further evidence that this reanchoring is appropriate comes from GD's results for the relative sodium cation affinities of phenylalanine (Phe) and tryptophan (Trp), which are determined to lie 28.8 ± 6 and 35.8 ± 6 kJ/mol above that of Na^+(Ala). Na^+(Ala), in turn, has been determined to lie 8.1 kJ/mol above Na^+(Gly). The kinetic method studies of KOW find relative values of 31.6 ± 4 and 42.9 ± 4 kJ/mol for Phe and Trp, respectively, with a difference of 5.7 kJ/mol between Na^+(Ala) and Na^+(Gly). When these relative values are anchored to the Na^+(Gly) BDE of 161 kJ/mol, this gives the reported absolute ΔH_{298} values for Na^+(Ala), Na^+(Phe), and Na^+(Trp) of 169 ± 12, 198 ± 12, and 205 ± 12 kJ/mol, respectively, from GD and 167 ± 8, 198 ± 8, and 210 ± 8 kJ/mol, respectively, from KOW. (In this respect, it worth noting that the relative values of KOW were converted to an absolute scale by using acetamide, *N*-methylacetamide, and *N*,*N*-dimethylacetamide as references, whose absolute sodium cation affinities were established using theory rather than experiment.) Reanchoring to 166 kJ/mol for Na^+(Gly) moves the values for Na^+(Phe) and Na^+(Trp) to 203 ± 12 and 210 ± 12 (GD) and 203 ± 8 and 215 ± 8 (KOW) kJ/mol, respectively. These latter values agree better with the absolute values of 208.3 ± 6.8 and 220.0 ± 7.7 kJ/mol, respectively, determined using TCID methods by Ruan and Rodgers.[64] A reviewer suggests that the GD results should be anchored to an absolute value for Na^+(pyridine) taken from Amunugama and Rodgers,[65] as this molecule was used to measure the equilibrium values with Gly, Ala, and *o*-methylalanine (MeAla), where the latter were then used in equilibrium experiments with several other amino acids including Pro. This would lead to absolute sodium cation affinities at 298 K of 152 ± 9 kJ/mol for Gly, 166 ± 12 kJ/mol for Pro, 189 ± 12 kJ/mol for Phe, and 196 ± 12 kJ/mol for Trp. Compared to the absolute values measured by TCID measurements, these values are lower by 14, 20, 19, and 24 kJ/mol (an average of 19 ± 4 kJ/mol). It would appear that the use of pyridine as a primary anchor is not particularly effective in these studies. This is probably a result of the large enthalpy differences for Na^+ binding of pyridine compared to Gly, Ala, and MeAla, as well as the appreciable entropic differences between complexation of the multidentate amino acids and monodentate pyridine by Na^+. As the equilibrium studies require adjusting the directly measured free energies to enthalpies using calculated entropies, large entropy differences may not be handled correctly whereas the use of similar ligands allows for more effective cancellation of errors.

GD originally postulated that the reason their value for Na^+(Pro) was so much lower than that of KOW might be because they studied a higher energy conformation (suggested to be the charge solvated structure rather than the zwitterionic complex). In this rationalization, GD suggest that the proline complex is unable to access the zwitterionic structure during the equilibrium ligand exchange process. This rationalization could only hold if the ligand exchange reactions form the M1 complex predominantly as MRT have calculated a large barrier (~80 kJ/mol) for conversion from the M1 to ZW of Pro for all three alkali cations.[13] Formation of M1 as the primary species seems very unlikely because the N2 lowest energy conformation of neutral proline should be able to form the M3 complex with all three of the alkali cations without requiring any rearrangement of the ligand. Once M3 is formed, our calculations show that the M3 complex spontaneously rearranges by a simple H atom transfer to form the ZW isomer. This is consistent with the fact that no evidence for the M1 complex is found in the spectroscopic studies of KLMO.[10] In any event, the rationalization of GD is unnecessary as the present results are consistent with their equilibrium thermochemistry, especially if reanchored. Given the relative bond energies for Na^+(Gly) and Na^+(Pro) measured in the three laboratories, it seems likely that the result for Na^+(Pro) of KOW is somewhat high, possibly because of entropic effects associated with conversion of the zwitterionic ligand in the complexes to a nonzwitterionic neutral proline molecule upon dissociation at the higher excitation energies needed for the kinetic method. (A reviewer suggests that such entropic effects might also plague the TCID results to a lesser extent, but this fails to recognize that our analysis of the kinetic energy dependent cross sections includes a complete molecular description of the energized molecule and the transition state for dissociation, such that entropic effects are explicitly included. Further, in TCID experiments, any entropic effects are second order effects because they only change the kinetic shift and cannot influence the true threshold energy. It is possible that failure to properly include the symmetry number for an internal rotor or some related problem could introduce an entropic effect

not covered by our analysis,[40] but the proline system in particular should have none of these problems, as described above. Even in other systems where such problems might exist, the variations in the frequencies and time scale for dissociation used to determine absolute uncertainties in our thermochemical information encompass any uncertainties in such entropy effects. In the case of Na^+(Pro), for instance, we verified that an unaccounted entropic effect of a factor of 10 would still lie within the uncertainties already listed.) It is also possible that in the bis-ligated (AA)M^+(Pro) complexes studied by KOW, steric restrictions change the structure of the proline ligand such that formation of the M^+(Pro) low energy complex is not easily achieved upon dissociation of the other amino acid (AA) ligand. A reviewer suggests that such an effect could also explain why the equilibrium results of GD do not access the ZW state of Na^+(Pro), although this explicitly postulates that a true equilibrium is not achieved, whereas there is no indication that this is true in the results of GD. In contrast, because kinetic method experiments are done at elevated (and unknown) energies or temperatures to allow an appreciable dissociation signal, the relative probabilities of the competitive dissociations can be controlled by entropic effects much more readily.

The KLMO study measures the vibrational IR spectra of gas-phase Na^+(Pro) complexes and provides direct evidence for formation of the zwitterionic complex.[10] For the proline complex, no evidence of the formation of the M1 or any other nonzwitterionic structure was observed. In the same study, the M1 complex of Na^+(Gly) was found to be dominant, but a mixture of other isomers (including the ZW) could not be ruled out. The gas phase ions for the vibrational measurements were prepared using MALDI. It is possible that our complexes, formed in the DC/FT, have a different distribution of isomers present; however, the KLMO study clearly shows that the principal conformations in the Na^+ complexes of Pro and Gly are ZW and M1, respectively, in agreement with the theoretical predictions for the lowest energy conformations, which agree with the bond energies measured by TCID.

Feng, Gronert, and Lebrilla (FGL)[66] have reported an experimental ΔG_{298} value for Li^+(Pro) of 199 ± 13 kJ/mol obtained using the kinetic method, 49 ± 17 kJ/mol lower than our reported ΔG_{298} value of 248 ± 11 kJ/mol, Table 7, and also much lower than the theoretical values which range from 218 to 235 kJ/mol, Tables 6 and 7. The FGL values are anchored to Li^+ binding affinities of dimethylformamide, methylacetamide, and dimethylacetamide reported by Burk et al.[67] They also obtain a ΔG_{298} value for Li^+(Gly) of 174 ± 13 kJ/mol, 20 ± 18 kJ/mol lower than a TCID value from our lab of 194 ± 12 kJ/mol.[68] Using our Li^+(Gly) value as an anchor leads to slightly better agreement between the FGL value for Li^+(Pro) and the one reported here. FGL do note that their Li^+(Pro) binding energy is unusually low relative to KOW's measurement of the Na^+(Pro) binding energy, given the trends observed for Li^+ and Na^+ binding energies to amino acids with alkyl side chains. FGL hypothesize that one possible explanation for this low Li^+(Pro) binding energy is that they have formed the nonzwitterionic Li^+(Pro) complex; however, the large discrepancy is inconsistent with their calculations at the CISD(T)/6-31+G(d,p)//MP2/6-31+G(d) level, which only favor the zwitterion by 3 kJ/mol relative to the M1 structure, or ours where the calculated difference is 13−14 kJ/mol (Table 5).

Comparison to Theoretical Literature Values. The M^+(Pro) (M^+ = Li^+, Na^+, and K^+) systems have been theoretically examined by Marino, Russo, and Toscano (MRT).[13] MRT examine multiple structures in these systems and the transition states between them using geometries optimized at the B3LYP/6-311++G(d,p) level. Single-point energies for the optimized structures were calculated using the DFT methodology with a number of different exchange and correlation functionals. The lowest energy structures for each metal system were found to be the ZW conformation and the ordering of the higher energy M1 and M3 isomers agree with the results presented here. As shown in Table 6, the range of values presented by MRT tend to agree most closely to our DFT calculations at the B3LYP/6-311+G(2d,2p)//B3LYP/6-311G(d,p) level. The MRT values underestimate the experimental value of Li^+(Pro) reported here, 279 ± 10 kJ/mol, by an average of 11 ± 3 kJ/mol, although the larger values are within experimental error. The trend is reversed for Na^+(Pro), with the MRT calculations overestimate our experimental binding energy, 186 ± 4 kJ/mol, by an average of 12 ± 3 kJ/mol. For the K^+(Pro) system, our experimental and the MRT theoretical values are in good agreement with an average difference of 2 ± 2 kJ/mol.

KOW also report theoretical calculations for Na^+(Pro) at the MP2(full)/6-311+G(2d,2p)//MP2(full)/6-31G(d) level without BSSE corrections, obtaining a 298 K value of 195 kJ/mol. This agrees well with our own calculations using at the MP2(full)/6-311+G(2d,2p)//B3LYP/6-311G(d,p) level without BSSE, which also give a 298 K value of 195 kJ/mol (Tables 6 and 7). Likewise, GD calculated a 298 K value of 191 kJ/mol at the B3P86/6-311+G(2df,2pd)//B3P86/6-31+G(d,p) level where the geometry optimizations used an expanded basis set of 6-311+G(d) on Na. Our B3P86/6-311+G(2d,2p)//B3LYP/6-311G(d,p) result is comparable, 193 kJ/mol at 298 K (Tables 6 and 7). These authors also found that the nonzwitterionic complex geometry lay 27 kJ/mol higher in energy than the zwitterionic complex, comparable to the differences obtained here of about 22 kJ/mol at all three levels of theory explored (Table 4). Lau et al. have reported a theoretical value for the K^+(Pro) bond energy at 298 K of 143 kJ/mol using a B3LYP/6-311G(3df,2p)//B3LYP/6-31G(d) level of theory,[7] the same as our B3LYP value of 143 kJ/mol (Tables 6 and 7). Talley et al.[53] have reported relative (but not absolute) theoretical binding energies for the complexes of Pro bound to Li^+, Na^+, and K^+ using the MP2(full)/6-311+G(2d,2p)//MP2(full)/6-31G(d) level. Their results show the zwitterionic form to be the lowest energy complex in all cases, consistent with the results reported here. At the MP2(full)/6-31G(d) level of geometry optimization, the M3 structures for Li^+ and Na^+ converge into the ZW structure. This conversion involves a simple proton transfer of the carboxylic acid OH hydrogen to the amine nitrogen. As discussed in detail above, our calculations at the B3LYP/6-311G(d,p) level find a stable minimum for the M3 conformation but show that the barrier for the proton transfer between the M3 and ZW conformations is quite small and disappears once zero-point energies are included. The energies for M1 relative to the ZW conformation reported by Talley are on average 5 ± 1 kJ/mol higher than the values reported here (Table 4).

Trends in Metal Ion Affinities. Experimental results show that Li^+, Na^+ and K^+ bind more strongly to Pro relative to Pip by 6.7, 1.9, and 8.7 kJ/mol, respectively. Theoretical results for Na^+ and K^+ exhibit the same trend with Pro binding more strongly by 1.0 ± 0.3 kJ/mol and by 1.3 ± 2.2 kJ/mol, respectively. For Li^+, theory predicts the opposite trend with Pip binding more strongly by 6.8 ± 1.3 kJ/mol. The preference for the five-membered ring occurs despite Pip having an additional carbon atom to provide a higher polarizability and, consequently, an increase in binding strength. For comparison, experimental binding energies for glycine and alanine, amino

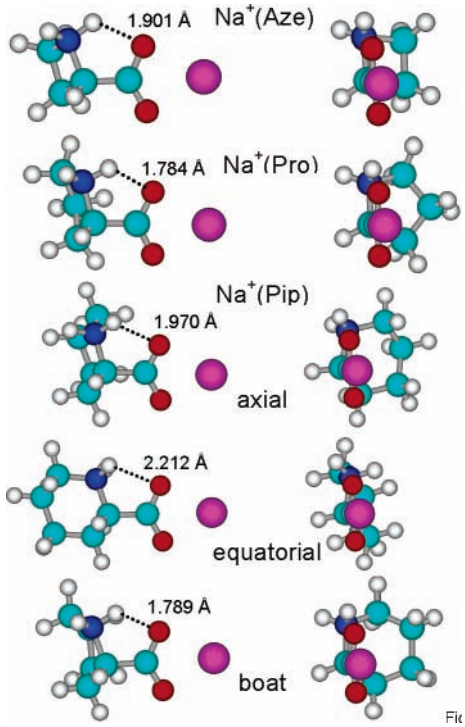

Figure 9. Side and top views of the low energy structures calculated for Na^+(Aze), Na^+(Pro), and Na^+(Pip). Axial, equatorial, and boat conformations are shown for Na^+(Pip). The N−H···O═C hydrogen bond lengths are provided in all cases.

acids that also differ by a single carbon atom, show the Na^+(Ala) binding energy is 6 and 8 kJ/mol[8,9] greater than that of Na^+(Gly).

Viewing the structure of the metal ion binding to these ligands (see for example the Na^+ complexes shown in Figure 9) shows how the metal ion, oxygen atoms, and the amine hydrogen form a planar structure in the Na^+(Pro) complex, which is also the case for Li^+(Pro) and K^+(Pro). This diagram illustrates that the N−H···O═C hydrogen bond is considerably shorter in the Pro complex and also more planar. Indeed, the zwitterionic form of M^+(Pro) has a particular advantage because this hydrogen bond forms without energetically unfavorable deformations to the ring structure. The lack of conformational flexibility in the four-membered analogue, azetidine-2-carboxcylic acid, restricts the hydrogen bond to being longer than that in the proline complex. Although the six-membered analogue, pipecolic acid, has more structural flexibility, the ring prefers a chair conformation, which prevents it from directing the amide hydrogen toward the carboxylate. Figure 9 shows that the axial conformation achieves a shorter and more planar hydrogen bond than the equatorial conformation, but to have a bond almost as short and as planar as that in the M^+(Pro) complex, the six-membered ring must distort to a boat conformation, which requires even more energy, Table 5.

All levels of theory for all of the systems studied here predict that the zwitterion is the most stable complex. This is because the high proton affinity of the secondary amine results in an intramolecular hydrogen bond between the amine hydrogen and the carboxylic acid with exceptional strength. Comparison of the experimental bond energies with the calculated values confirms that this zwitterionic complex is being examined in all cases.

It is notable that all of the factors that affect the stability of these complexes work in the positive direction for proline, making the five-membered ring ideal for chelating a metal cation. This allows proline to bind to the alkali metal cations with a strength outside the trend exhibited by the other amino acids with aliphatic side chains. Its cyclic structure results in proline being difficult to categorize among the 20 naturally occurring amino acids, and the results presented here reveal that the five-membered ring itself has unique properties. These factors may provide some insight into why the five-membered ring evolved as the only cyclic naturally occurring amino acid.

Acknowledgment. Funding for this work was provided by the National Science Foundation under Grant CHE-0135517 and 0451477. An allocation of computer time from the Center for High Performance Computing at the University of Utah is gratefully acknowledged.

Supporting Information Available: Three tables of vibrational frequencies, average vibrational energies at 298 K, rotational constants, and Cartesian coordinates of the neutral molecules and alkali metal complexes determined at the B3LYP/6-311G(d,p) level. This material is available free of charge via the Internet at http://pubs.acs.org.

References and Notes

(1) Vitagliano, L.; Berisio, R.; Mastrangelo, A.; Mazzarella, L.; Zagari, A. *Protein Sci.* **2001**, *10*, 2627−2632.
(2) Stepanian, S. G.; Reva, I. D.; Radchenko, E. D.; Adamowicz, L. *J. Phys. Chem. A* **2001**, *105*, 10664−10672.
(3) Moision, R. M.; Armentrout, P. B. *J. Phys. Chem. A* **2002**, *106*, 10350−10362.
(4) Moision, R. M.; Armentrout, P. B. *Phys. Chem. Chem. Phys.* **2004**, *6*, 2588−2599.
(5) Hoyau, S.; Ohanessian, G. *Chem. Eur. J.* **1998**, *4*, 1561.
(6) Hoyau, S.; Norrman, K.; McMahon, T. B.; Ohanessian, G. *J. Am. Chem. Soc.* **1999**, *121*, 8864−8875.
(7) Lau, J. K.-C.; Wong, C. H. S.; Ng, P. S.; Siu, F. M.; Ma, N. L.; Tsang, C. W. *Chem. Eur. J.* **2003**, *9*, 3383−3396.
(8) Kish, M. M.; Ohanessian, G.; Wesdemiotis, C. *Int. J. Mass Spectrom.* **2003**, *227*, 509−524.
(9) Gapeev, A.; Dunbar, R. C. *Int. J. Mass Spectrom.* **2003**, *228*, 825−839.
(10) Kapota, C.; Lemaire, J.; Maître, P.; Ohanessian, G. *J. Am. Chem. Soc.* **2004**, *126*, 1836−1842.
(11) Nguyen, D. T.; Scheiner, A. C.; Andzelm, J. W.; Sirois, S.; Salahub, D. R.; Hagler, A. T. *J. Comput. Chem.* **1997**, *18*, 1609−1631.
(12) Feng, W. Y.; Gronert, S.; Lebrilla, C. B. *J. Phys. Chem. A* **2003**, *107*, 405−410.
(13) Marino, T.; Russo, N.; Toscano, M. *J. Phys. Chem. B* **2003**, *107*, 2588−2594.
(14) Ervin, K. M.; Armentrout, P. B. *J. Chem. Phys.* **1985**, *83*, 166−189.
(15) Muntean, F.; Armentrout, P. B. *J. Chem. Phys.* **2001**, *115*, 1213−1228.
(16) Dalleska, N. F.; Honma, K.; Armentrout, P. B. *J. Am. Chem. Soc.* **1993**, *115*, 12125−12131.
(17) Dalleska, N. F.; Tjelta, B. L.; Armentrout, P. B. *J. Phys. Chem.* **1994**, *98*, 4191−4195.
(18) Fisher, E. R.; Kickel, B. L.; Armentrout, P. B. *J. Phys. Chem.* **1993**, *97*, 10204−10210.
(19) Khan, F. A.; Clemmer, D. E.; Schultz, R. H.; Armentrout, P. B. *J. Phys. Chem.* **1993**, *97*, 7978−7987.
(20) Schultz, R. H.; Crellin, K. C.; Armentrout, P. B. *J. Am. Chem. Soc.* **1991**, *113*, 8590−8601.
(21) Rodgers, M. T.; Armentrout, P. B. *J. Phys. Chem. A* **1997**, *101*, 1238−1249.
(22) Teloy, E.; Gerlich, D. *Chem. Phys.* **1974**, *4*, 417−427.
(23) Gerlich, D. *Adv. Chem. Phys.* **1992**, *82*, 1−176.
(24) Aristov, N.; Armentrout, P. B. *J. Phys. Chem.* **1986**, *90*, 5135.
(25) Dalleska, N. F.; Honma, K.; Sunderlin, L. S.; Armentrout, P. B. *J. Am. Chem. Soc.* **1994**, *116*, 3519−3528.
(26) Beyer, T. S.; Swinehart, D. F. *Commun. Assoc. Comput. Machinery* **1973**, *16*, 379.
(27) Stein, S. E.; Rabinovich, B. S. *J. Chem. Phys.* **1973**, *58*, 2438.
(28) Stein, S. E.; Rabinovich, B. S. *Chem. Phys. Lett.* **1977**, *49*, 1883−1888.
(29) Gilbert, R. G.; Smith, S. C. *Theory of Unimolecular and Recombination Reactions*; Blackwell Scientific: London, 1990.
(30) Rodgers, M. T.; Ervin, K. M.; Armentrout, P. B. *J. Chem. Phys.* **1997**, *106*, 4499.

(31) Rodgers, M. T.; Armentrout, P. B. *J. Phys. Chem. A* **1997**, *101*, 2614−2625.

(32) DeTuri, V. F.; Ervin, K. M. *J. Phys. Chem. A* **1999**, *103*, 6911−6920.

(33) More, M. B.; Ray, D.; Armentrout, P. B. *J. Phys. Chem. A* **1997**, *101*, 7007−7017.

(34) More, M. B.; Glendening, E. D.; Ray, D.; Feller, D.; Armentrout, P. B. *J. Phys. Chem.* **1996**, *100*, 1605−1614.

(35) More, M. B.; Ray, D.; Armentrout, P. B. *J. Am. Chem. Soc.* **1999**, *121*, 417−423.

(36) Ray, D.; Feller, D.; More, M. B.; Glendening, E. D.; Armentrout, P. B. *J. Phys. Chem.* **1996**, *100*, 16116−16125.

(37) Rodgers, M. T.; Armentrout, P. B. *J. Phys. Chem. A* **2000**, *104*, 2238−2247.

(38) Rodgers, M. T.; Armentrout, P. B. *J. Phys. Chem. A* **1999**, *103*, 4955−4963.

(39) Amicangelo, J. C.; Armentrout, P. B. *J. Phys. Chem. A* **2000**, *104*, 11420−11432.

(40) Amicangelo, J. C.; Armentrout, P. B. *Int. J. Mass Spectrom.* **2001**, *212*, 301−325.

(41) Chantry, P. J. *J. Chem. Phys.* **1971**, *55*, 2746−2759.

(42) Armentrout, P. B. In *Advances in Gas-Phase Ion Chemistry*; Adams, N. G., Babcock, L. M., Eds.; JAI Press Inc.: Greenwich, CT, 1992; Vol. 1, p 83.

(43) Armentrout, P. B.; Simons, J. *J. Am. Chem. Soc.* **1992**, *114*, 8627.

(44) Frisch, M. J.; Trucks, G. W.; Schlegel, H. B.; Scuseria, G. E.; Robb, M. A.; Cheeseman, J. R.; Montgomery, J. A., Jr.; Vreven, T.; Kudin, K. N.; Burant, J. C.; Millam, J. M.; Iyengar, S. S.; Tomasi, J.; Barone, V.; Mennucci, B.; Cossi, M.; Scalmani, G.; Rega, N.; Petersson, G. A.; Nakatsuji, H.; Hada, M.; Ehara, M.; Toyota, K.; Fukuda, R.; Hasegawa, J.; Ishida, M.; Nakajima, T.; Honda, Y.; Kitao, O.; Nakai, H.; Klene, M.; Li, X.; Knox, J. E.; Hratchian, H. P.; Cross, J. B.; Adamo, C.; Jaramillo, J.; Gomperts, R.; Stratmann, R. E.; Yazyev, O.; Austin, A. J.; Cammi, R.; Pomelli, C.; Ochterski, J. W.; Ayala, P. Y.; Morokuma, K.; Voth, G. A.; Salvador, P.; Dannenberg, J. J.; Zakrzewski, V. G.; Dapprich, S.; Daniels, A. D.; Strain, M. C.; Farkas, O.; Malick, D. K.; Rabuck, A. D.; Raghavachari, K.; Foresman, J. B.; Ortiz, J. V.; Cui, Q.; Baboul, A. G.; Clifford, S.; Cioslowski, J.; Stefanov, B. B.; Liu, G.; Liashenko, A.; Piskorz, P.; Komaromi, I.; Martin, R. L.; Fox, D. J.; Keith, T.; Al-Laham, M. A.; Peng, C. Y.; Nanayakkara, A.; Challacombe, M.; Gill, P. M. W.; Johnson, B.; Chen, W.; Wong, M. W.; Gonzalez, C.; Pople, J. A. *Gaussian 03*, revision B.02; Gaussian, Inc.: Pittsburgh, PA, 2003.

(45) Pearlman, D. A.; Case, D. A.; Caldwell, J. W.; Ross, W. R.; Cheatham, T. E.; DeBolt, S.; Ferguson, D.; Seibel, G.; Kollman, P. *Comput. Phys. Commun.* **1995**, *91*, 1−41.

(46) High Performance Computational Chemistry Group, NWChem, A Computational Chemistry Package for Parallel Computers, 4.5, Pacific Northwest National Laboratory, Richland, WA 99352, 2003.

(47) Montgomery, J. A., Jr.; Frisch, M. J.; Ochterski, J. W.; Petersson, G. A. *J. Chem. Phys.* **1999**, *110*, 2822.

(48) van Duijneveldt, F. B.; van Duijneveldt de Rijdt, J. G. C. M.; van Lenthe, J. H. *Chem. Rev.* **1994**, *94*, 1873−1885.

(49) Wong, C. H. S.; Siu, F. M.; Ma, N. L.; Tsang, C. W. *THEOCHEM* **2002**, *588*, 9−16.

(50) Feller, D.; Glendening, E. D.; Woon, M. W.; Feyereisen, J. *J. Chem. Phys.* **1995**, *103*, 3526.

(51) Feller, D. *Chem. Phys. Lett.* **2000**, *322*, 543.

(52) McMahon, T. B.; Ohanessian, G. *Chem. Eur. J.* **2000**, *6*, 2931−2941.

(53) Talley, J. M.; Cerda, B. A.; Ohanessian, G.; Wesdemiotis, C. *Chem. Eur. J.* **2002**, *8*, 1377−1388.

(54) Lifshitz, C. *Adv. Mass Spectrom.* **1989**, *11*, 713−729.

(55) Peng, C. Y.; Schlegel, H. B. *Isr. J. Chem.* **1994**, *33*, 449.

(56) Solomons, T. W. G. *Orgainc Chemistry*, 5th ed.; Wiley: New York, 1992.

(57) Peng, C. Y.; Ayala, P. Y.; Schlegel, H. B.; Frisch, M. J. *J. Comput. Chem.* **1996**, *17*, 49.

(58) Armentrout, P. B.; Rodgers, M. T. *J. Phys. Chem. A* **2000**, *104*, 2238−2247.

(59) Rodgers, M. T.; Armentrout, P. B. *J. Am. Chem. Soc.* **2000**, *122*, 8548−8558.

(60) Rodgers, M. T. *J. Phys. Chem. A* **2001**, *105*, 8145−8153.

(61) Yang, Z.; Rodgers, M. T. *J. Am. Chem. Soc.*, in press.

(62) Rodgers, M. T.; Armentrout, P. B. Work in progress.

(63) Curtiss, L. A.; Raghavachari, K.; Redfern, P. C.; Rassolov, V.; Pople, J. A. *J. Chem. Phys.* **1998**, *109*, 7764−7776.

(64) Ruan, C.; Rodgers, M. T. *J. Am. Chem. Soc.* **2004**, *126*, 14600−14610.

(65) Amunugama, R.; Rodgers, M. T. *J. Phys. Chem. A* **2001**, *105*, 9883−9892.

(66) Feng, W. Y.; Gronert, S.; Lebrilla, C. B. *J. Am. Chem. Soc.* **1999**, *121*, 1365−1371.

(67) Burk, P.; Koppel, I. A.; Koppel, I.; Kurg, R.; Gal, J.-F.; Maria, P.-C.; Herreros, M.; Notario, R.; Abboud, J.-L. M.; Anvia, F.; Taft, R. W. *J. Phys. Chem. A* **2000**, *104*, 2824−2833.

(68) Moision, R. M.; Armentrout, P. B. Work in progress.